MEASUREMENT UNCERTAINTIES IN GAS-BASED MONITORS FOR HIGH REPETITION RATE X-RAY FEL OPERATIONS*

Y. Feng#, J. Krzywinski, M. Campell, D. W. Schafer, E. Ortiz, M. Rowen, T. O. Raubenheimer,
SLAC, Menlo Park, CA 94025, USA

Abstract

Thermodynamic simulations using a finite difference method were carried out to investigate the measurement uncertainties in gas-based X-ray FEL diagnostic monitors under high repetition rate operations such as planned for the future LCLS-II soft and hard X-ray FEL's. For monitors using relatively high gas pressures for obtaining sufficient signals, the absorbed thermal power becomes non-negligible as repetition rate increases while keeping pulse energy constant. The fluctuations in the absorbed power were shown to induce significant measurements uncertainties, especially in the single-pulse mode. The magnitude of this thermal effect depends nonlinearly on the absorbed power and can be minimized by using a more efficient detection scheme in which the gas pressure can be set sufficiently low.

INTRODUCTION

The Linac Coherent Light Source (LCLS) currently operating at SLAC National Accelerator Laboratory will soon start to construct, under the LCLS-II project, a new 4 GeV continuous-wave (CW) superconducting radio frequency (SCRF) linear accelerator, in addition to the existing normal conducting RF Cu linac (CuRF). There will be two new variable-gap undulators to be placed in the existing LCLS undulator tunnel: a new soft X-ray undulator and a hard X-ray undulator that would replace the existing LCLS fixed-gap undulator. Both new undulators, when fed by the SCRF linac, could run at a very high repetition rate up to ~ 1 MHz, nearly 4 orders of magnitude higher than the LCLLS 120 Hz operation. Both undulators will operate in the Self Amplified Spontaneous Emission [1] (SASE) mode with the option to be self-seeded over certain energy ranges. Due to the intrinsic stochastic nature of the SASE lasing process and other extrinsic random mechanisms in the linac, many important parameters of the FEL beam fluctuate randomly from pulse to pulse [2]. For example, the pulse intensity can vary by as much as a 10% in the SASE mode to nearly 100% in the seeded mode [3]. Many diagnostic devices are needed to help the accelerator operators to optimize the lasing performance, and to enable the users to normalize the experimental data [4-8].

The various diagnostic devices are typically located in the Front-End Enclosure (FEE) just downstream of the undulator but upstream of any experimental endstations. They are often required to be highly transmissive and minimally intrusive as to introduce only negligible wavefront distortion or transverse coherence degradation. Because of the close proximity of FEE to the effective source location, which is somewhere between the FEL saturation point and the end of undulators (EOU), the power density of the beam at the device locations is quite high, and the diagnostic devices must be based on using a gas medium or a thin solid film to avoid damages while assuring the transmission requirement. For soft X-ray FEL beams in particular, gas-based concepts are the only viable solutions because of the high absorption cross-section at these energies even for the very low *Z* materials. For pulse energy measurement, LCLS-II is planning to install two Gas Detector Monitors [9] (GMD's), one of the original design for very soft X-rays and another the latest version specifically optimized for covering higher X-ray energies, on the soft X-ray transport line in the FEE for the SCRF high repetition rate FEL beam. Both GMD's should be capable of providing pulse-to-pulse measurements at greater than 1 MHz repetition rate, but would require very low operating pressures on the order of only 10^{-5} hPa because of the highly efficient direct detection of the ions/electrons from photoionization by the impinging FEL beam.

On the LCLS-II hard X-ray transport line in the FEE, the existing LCLS N_2 gas energy detectors [10] (GED's) shown in Figure 1 will be re-purposed with upgrades for providing pulse-to-pulse measurements of both the high repetition rate FEL when driven by the SCRF linac as well as the 120 Hz high pulse energy FEL when driven by the CuRF linac. The GED concept is based on the detection of the near ultraviolet (UV) optical radiation from the N_2 molecules excited by the secondary electrons, which are produced by the primary photoelectron via collisions with the N_2 molecules. This indirect radiation process in a GED, in contrast to what happens in a GMD, is far less efficient, and thus requires the use of a much higher operation pressure of order 0.01 to 1 hPa, an increase of 3 to 5 orders of magnitude.

Gas-based systems such as the gas attenuator used for LCLS and also being planned for LCLS-II, however, have been shown to exhibit density depression or the so-called "filamentation" effect [11], when the energy absorbed in the gas medium is sufficiently high so that it can no longer be considered as being merely a small perturbation. The effective attenuation not only depends on the pressure, but also on many other physical attributes of the attenuator system itself, including gas type and it thermal properties, the length and radius of the gas tube, the transverse profile of the FEL beam [12]. If the input pulse energy fluctuates as in any SASE based FEL pulses, the attenuation received by any given pulse also varies substantially but in a delayed and hysteric manner and is

*Work supported by DOE under Contract #. DE-AC02-76SF00515.
#yfeng@slac.stanford.edu

ISBN 978-3-95450-134-2

essentially not predictable [13]. This non-deterministic behaviour presents a rather serious operational challenge to the users and could cause irreparable damages to equipment that the attenuator is designed to protect. One of the mitigation strategies is to measure the attenuated intensity by a separate diagnostic device and use it as a feedback to make the proper adjustment to the operating pressure to obtain the requirement attenuation.

Since the downstream intensity diagnostic device is also gas based, a similar filamentation or density depression effect is expected to be present, which would in turn impact the measurement as well. As stated earlier, for gas-based energy monitors the absorbed energy is typically designed to be very small, although in the case of GED it is not entirely negligible because of the higher operating pressure to compensate for the lower light production efficiency. In this report, we will investigate the uncertainties in the pulse intensity measurement using a GED under the LCLS-II high repetition rate operations, especially when the input pulse energy thus the running average of the input power fluctuates randomly. It was found that these random variations would lead to significant measurements uncertainties on a pulse-by-pulse basis. The magnitude of this thermal effect depends nonlinearly on the averaged absorbed power and can be minimized by using a more efficient detection scheme such as that of the GMD's, for which the gas pressure can be set sufficiently low.

GAS MONITORS SIMULATIONS

The ultrafast interaction between the FEL pulses and the gas atoms/molecules in a gas monitor is very complex and is the subject of many pioneering research activities ranging from nonlinear atomic and molecular science to FEL driven atomic X-ray lasers [14, 15], which often involving focusing the already small FEL beam down to an even tinier spot. However, in either a gas attenuator or an energy monitor and for the purpose of this investigation, the FEL beam is unfocused and the light-matter interaction remains linear, and can be modelled simply as an energy deposition mechanism via photoabsorption that takes place instantaneously upon arrival of each pulse, creating a local temperature and a simultaneous pressure gradient in the gas medium along the beam path while the global density remains unchanged. The pressure gradient in turn drives hydrodynamic motions of the atoms/molecules to establish a global pressure equilibrium, resulting in a density gradient coexisting with the temperature gradient. What ensues is a slow process at a few nanoseconds and longer time scales dominated by thermal diffusion, dissipating eventually all of the deposited energy. The time-dependent behaviour of this thermodynamic process after each pulse is used to predict what temperature and density profile the next trailing pulse would effectively "see", from which the responses such as the intensity of the near UV production in a GED can be determined and the extent to which the fluctuations in input pulse energy can impact the measurement accuracy can be evaluated.

Time-dependent Behaviour with Random Input Pulse Energies

The simulation techniques used to study the steady state and time dependent solutions of a gas attenuator [12,13] were used. Potential modifications for taking into account the specific GED geometry shown in Figure 1 and operating conditions turned out to be not necessary. Because of the relatively rare gas pressure, the temperature gradient along the beam direction remains small in comparison to that in the radial direction. As such the computational procedures developed earlier [13] can be readily applied here, whereby the time-dependent temperature and density profiles were obtained by solving a one-dimensional partial differential heat equation for a thin slab starting at the entrance of the gas pipe and repeating it sequentially towards the exit.

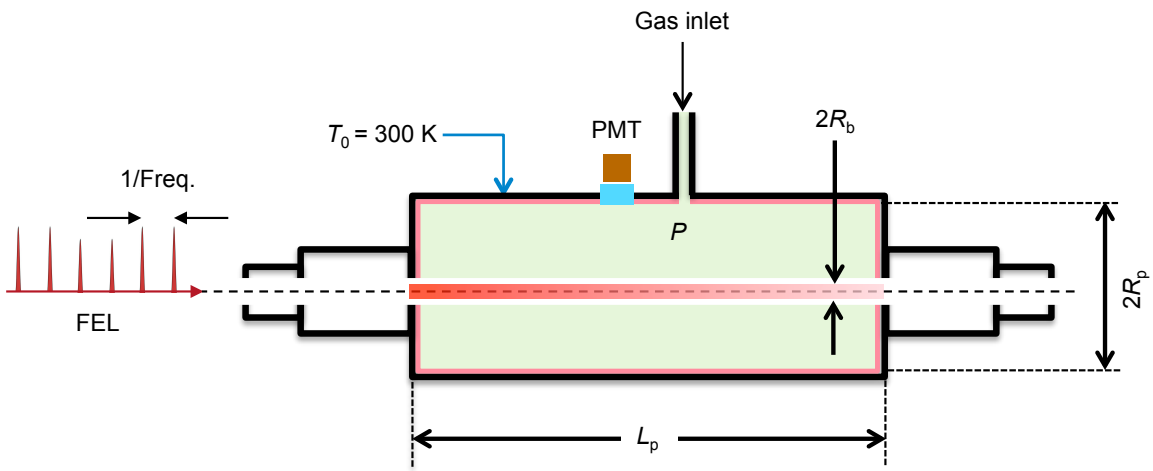

Figure 1: Schematic of the LCLS-II hard X-ray gas detector, consisting of a cylindrical pipe filled with N_2 gas bookended by two differential pumping sections. The pipe has a length L_p and diameter of $2R_p$, and the FEL beam $2R_b$. The wall of the pipe is cooled to 300 K, and the gas inlet maintains the pressure P ranging from tens of mTorr to a few Torr. The PMT is used to collect near UV radiation created by the passage of the FEL.

ISBN 978-3-95450-134-2

The simulation was done for a 1 keV X-ray FEL beam running at 100 kHz with an average per-pulse energy of 2 mJ distributed randomly from 0 to 4 mJ and an average power of 200 W. The energy of any given pulse was generated by using a standard pseudorandom scalar algorithm. The GED is 300 mm in length and 50 mm in diameter, with the outer wall cooled to 300 K, and the pressure P regulated to an equilibrium of 0.985 Torr to effectively attenuate the beam by 5%, about 2x higher than 0.345 Torr, which was calculated in the low-power limit when the filamentation effect due to the absorbed power is neglected. The gas pressure in the two differential pumping sections is assumed to be negligible as well. The isobaric specific heat of the N_2 gas was assumed to be constant at $7R/2$ due to it being in a fully excited rotational state but in the vibrational ground state, where R = 8.31 J/K·mol is the gas constant. In Figure 2, the time evolution of the temperature at the central entrance of the gas pipe is shown, exhibiting instantaneous rise immediately after the arrival of each pulse, and then a relaxation process towards the steady state value T_{eq} ~ 810 K, which depends on the average absorbed power Q in the gas volume. Because of the fluctuations in the input pulse energy, the asymptotic temperatures "seen" by the trailing pulses also vary randomly by as much as 150 K.

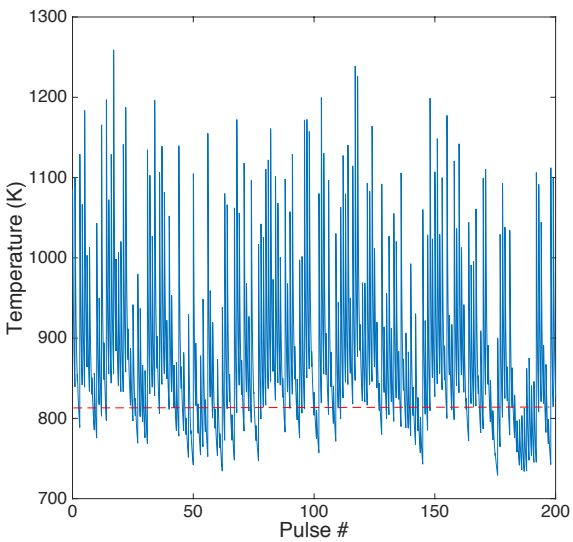

Figure 2: The time evolution of the temperature at the center of the entrance of the gas pipe as 200 random pulses of average energy of 2 mJ pass through. The targeted attenuation $A(0)$ was set for 0.05, resulting an average absorbed power of 10 W.

There are corresponding variations in the density distribution after each pulse, given by the assumed local equilibrium condition $n(r, z, t)T(r, z, t) = P/k_B$, where r, and z are the spatial coordinates, and P the equilibrium pressure [13] The actual achieved attenuation $A(Q)$ for any given pulse can be calculated from the density profile $n(r, z, t)$ and the photoabsorption cross-section of the N_2 gas and is plotted in Figure 3.

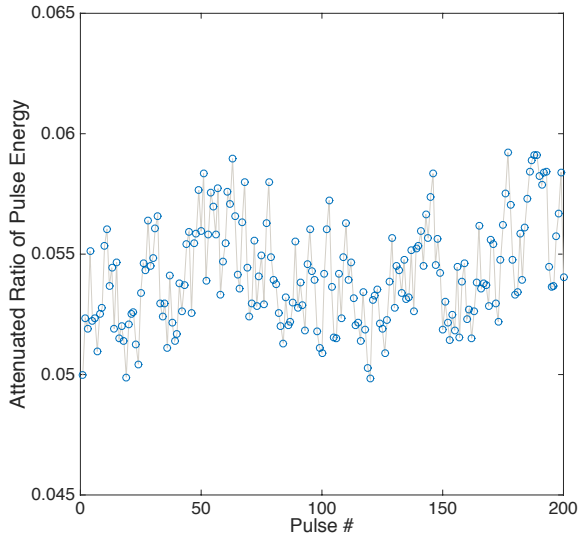

Figure 3: The actual received attenuation by each of the 200 pulses with randomly varying energy from 0 to 4 mJ. The targeted attenuation $A(0)$ was set for 0.05.

The achieved attenuation $A(Q)$ for any given pulse is no longer constant as expected in the low-power limit when the filamentation effect is negligible, and changes by as much as 20% peak-to-peak or 4.4% in standard deviation from the average value of 0.055, in addition, there is an overall shift of 0.005 in the average from the targeted value $A(0)$ of 0.05 to 0.055, reflecting the fact that the gas pressure was set a bit higher than required when using the result from the CW steady state simulation [13].

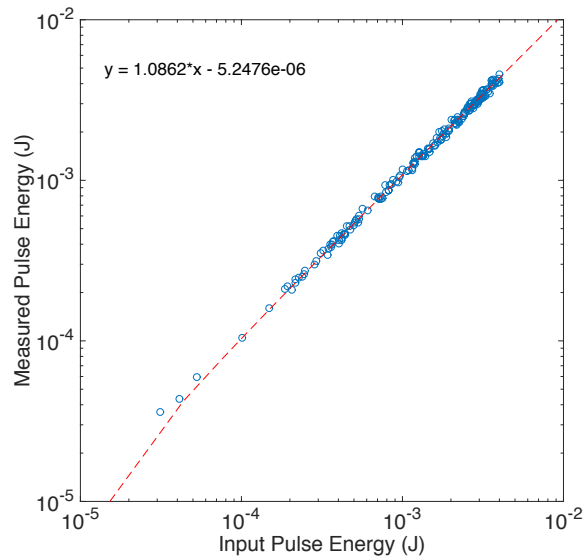

Figure 4: The measured pulse energy vs. the input pulse energy for the case that the effective attenuation is set for 5% or 10 W. The red dotted line is a linear fit.

Measured Pulse Energies

The photo multiplier tube (PMT) in Figure 1 is used to collect the near UV radiation generated indirectly by the

ISBN 978-3-95450-134-2

primary electrons via the photoabsorption process, which was assumed to be the dominant attenuation mechanism. The normalized pulse intensity measured by the PMT is proportional to the attenuated pulse energy, i.e., $I_m = I_0 \cdot A(Q) \cdot \eta / A(0)$, where I_0 is randomized input pulse energy, η is the quantum efficiency of the detector and is set to 1 for simplicity and for properly evaluating the measurement uncertainties, and $A(0)$ is the targeted attenuation in the low-power limit.

In Figure 4, the normalized measured pulse energy is plotted directly against the randomized input pulse energy, and a linear fit is also shown by the red dotted line. It can be seen that I_m correlates in general with the input energy I_0, but also exhibits substantive deviations that depend critically on the total power absorbed in the gas volume as evidenced by a similar simulation for $A(0)$ = 0.125% shown in Figure 5, where the deviations are greatly reduced, exemplifying the performance expected for an intensity monitor if the filamentation effect is absent.

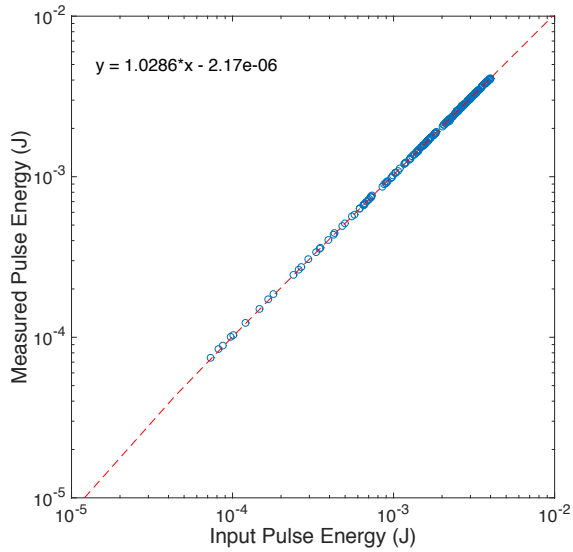

Figure 5: The measured pulse energy vs. the input pulse energy for the case that the effective attenuation is set for 0.125% or 0.25 W. The red dotted line is a linear fit.

Energy Measurement Uncertainties

To quantitatively assess the measurement uncertainties, the ratio of the measured over the input pulse energy is plotted against the input pulse energy in Figure 6 and Figure 7 for the 5% and 0.125% attenuation cases, respectively. The scatter in the data sets are markedly different, reaching as much as 20% peak-to-peak or σ = 4.3% in standard deviation for 5% or 10 W attenuation, but only 2.2% peak-to-peak, and 0.48% in σ for the 0.125% or 0.25 W attenuation. The ratios are both greater than unity because of the pressure settings were slightly higher than required in both cases, reflecting some small differences in steady state and time-dependent simulations in determining the equilibrium pressure [13]. This result is rather important since in order to reach the 1% relative accuracy requirement for pulse energy measurement, the absorbed power must be reduced to less than 0.5 W, and the attenuation to less than 0.25%. This finding will be used to help guide the LCLS N_2 gas detector upgrade to first emphasizing maximizing the near UV detection efficiency including more sensitive PMT's and lower electronics noise, thus reducing the required operating pressure. Additional gain can be made by reducing the pipe diameter to improve cooling of the gas molecules.

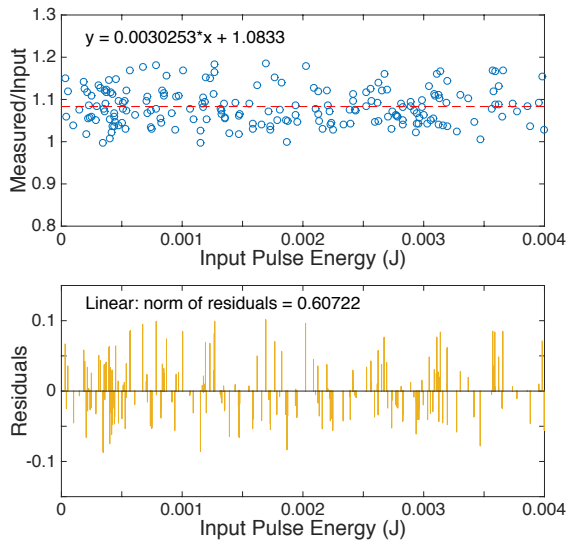

Figure 6: The ratio of the measured over the input pulse energy for the case that the effective attenuation is set for 5% or 10 W. The red dotted line is a linear fit, with the residuals shown in the bottom plot.

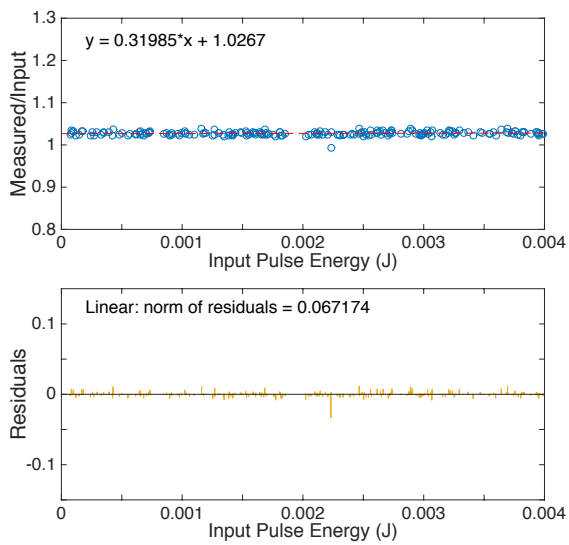

Figure 7: The ratio of the measured over the input pulse energy for the case that the effective attenuation is set for 0.125% or 0.25 W. The red dotted line is a linear fit, with the residuals shown in the bottom plot.

ISBN 978-3-95450-134-2

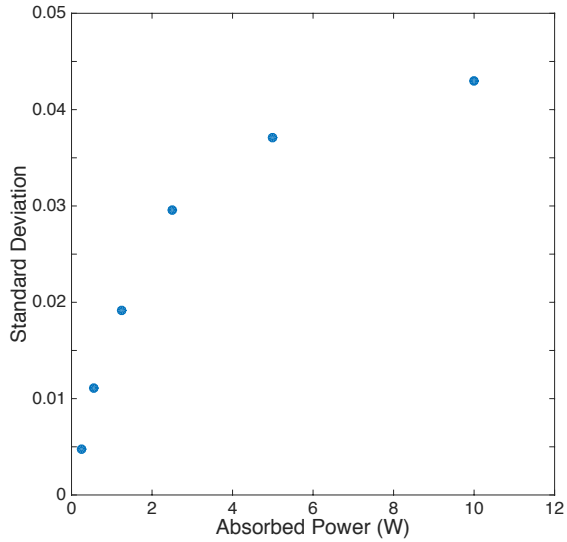

Figure 8: The dependence of the standard deviation σ for the pulse energy measurement on the power absorbed in the gas volume. The red dotted line is a polynomial fit. To achieve a relative accuracy of 1%, the power must be kept below 0.5 W given the specific design of the current LCLS N_2 gas detector.

CONCLUSION

We have carried out thermodynamic simulations to study the impact of filamentation effect on the measurement uncertainties in gas-based pulse energy monitors, when the absorbed power in the gas volume is not negligible. This is particularly applicable to the case of the LCLS-II N_2 gas detector under high repetition rate operations, in which the pressure or the density in the gas volume must be set sufficiently high to produce required signal strength for reliable measurements. It was found that the absorbed energy in the gas interaction volume exhibit random variations in response to the fluctuations in the input pulse energy as is the case for most SASE based FEL sources. Consequently, there could be substantial uncertainties in the pulse energy measurement, approaching 20% peak to peak or 4.3% in standard deviation, when the average absorbed power is set at 10 W. This undesirable effect can be minimized by devising more efficient monitoring technique whereby smaller gas pressure/density could be used, such as the GMD's planned for the soft X-ray transport line of the LCLS-II. For the GMD's, a potential issue could be the gas diffusion time being sufficiently short, since the ions and electrons generated from the photoabsorption process are designed to be swept from the interaction volume after each pulse, thus depleting the effective gas density. In principle, similar studies looking into the gas diffusion process in the GMD's should be performed. For other gas-based monitors designed for measurements other than energy such as capturing soft X-ray FEL single-shot spectra from analysing the kinetic energy of primary photoelectrons, the filamentation effect is expected to be not as important, because typically a gas jet is used, and the gas molecules in the interaction region are being replaced for every pulse.

ACKNOWLEDGMENT

Use of the Linac Coherent Light Source (LCLS), SLAC National Accelerator Laboratory, is supported by the U.S. Department of Energy, Office of Science, Office of Basic Energy Sciences under Contract No. DE-AC02-76SF00515.

REFERENCES

[1] A. M. Kondratenko, and E. L. and Saldin, Sov. Phys. Dokl. 24, 986 (1979); R. Bonifacio, C. Pellegrini, and L. M. Narducci, Opt. Commun. 50, 373 (1984).
[2] For example, E. L. Saldin, E. A. Schneidmiller, and M. V. Yurkov, Optics Communications 148, 383 (1998).
[3] P. Emma, private communication.
[4] Y. Feng, J. Feldkamp, D. M. Fritz, M. Cammarata, A. Robert, C. Caronna, H. T. Lemke, D. Zhu, S. Lee, S. Boutet, G. Williams, K. Tono, M. Yabashi, and J. Hastings, Proc. SPIE 8140, 81400Q (2011).
[5] For example, Bionta et al, Opt. Express 19, 21855 (2011).
[6] D. Zhu, M. Cammarata, J. M. Feldkamp, D. M. Fritz, J. B. Hastings, S. Lee, H. T. Lemke, A. Robert, J. L. Turner, and Y. Feng, Appl. Phys. Lett. 101, 034103 (2012).
[7] C. Behrens, et al, Nat. Comm. 5, 3762 (2014).
[8] E. Allaria, et al., Phys. Rev. X 4, 041040 (2014).
[9] K. Tiedtke et al. J. Appl. Phys. 103, 094511 (2008).
[10] S. P. Hau-Riege, R. M. Bionta, D. D. Ryutov, R. A. London, E. Ables, K. I. Kishiyama, S. Shen, M. A. McKernan, D. H. McMahon, M. Messerschmidt et al., Phys. Rev. Lett. 105, 043003 (2010).
[11] Y.-H. Cheng, J. K. Wahlstrand, N. Jhajj, and H.M. Milchberg, Optics Express 21, 4740 (2013).
[12] Y. Feng, J. Krzywinski, D. W. Schafer, E. Ortiz, M. Rowen, and T. O. Raubenheimer, submitted to J. Synch. Rad. (2015).
[13] Y. Feng, J. Krzywinski, D. W. Schafer, E. Ortiz, M. Rowen, and T. O. Raubenheimer, submitted to Proc. SPIE (2015).
[14] L. Young, E. P. Kanter, B. Krässig, Y. Li, A.M. March, S. T. Pratt, R. Santra, S. H. Southworth, N. Rohringer, L. F. DiMauro, et al., Nature 446, 56 (2010).
[15] N. Rohringer, D. Ryan, R. A. London, M. Purvis, F. Albert, J. Dunn, J. D. Bozek, C. Bostedt, A. Graf, R. Hill et al., Nature 481, 488 (2012).

ISBN 978-3-95450-134-2